

Optical and Electronic Properties of Molecular Systems Derived from Rhodanine

Duvalier Madrid-Úsuga,^{†,‡} Carlos A. Melo-Luna,^{†,‡} Alberto Insuasty,[¶] Alejandro Ortiz,^{†,§} and John H. Reina^{*,†,‡}

[†]*Centre for Bioinformatics and Photonics—CIBioFi, Cll. 13 No. 100-00, Edif. 320, Esp. 1069, Universidad del Valle, Cali 760032, Colombia*

[‡]*Department of Physics, Universidad del Valle, Cali 760032, Colombia*

[¶]*Department of Chemistry and Biology, Universidad del Norte, Km 5 via Puerto Colombia, Barranquilla 081007, Colombia*

[§]*Department of Chemistry, Universidad del Valle, Cali 760032, Colombia*

E-mail: john.reina@correounivalle.edu.co

Abstract

Push-Pull functional compounds consisting of dicyanorhodanine derivatives have attracted a lot of interest because their optical, electronic, and charge transport properties make them useful as building blocks for organic photovoltaic implementations. The analysis of the frontier molecular orbitals shows that the vertical transitions of electronic absorption are characterized as intramolecular charge transfer; furthermore, we show that the analyzed compounds exhibit bathochromic displacements when comparing the presence (or absence) of solvent as an interacting medium. In comparison with materials defined by their energy of reorganization of electrons (holes) as electron (hole) transporters, we find a transport hierarchy whereby the molecule (**Z**)-2-((1,1-dicyanomethylen)-5-(4-dimethylamino)benzylidene)-1,3-thiazole-4 is better at transport-

ing holes than molecule (**Z**)-2-((1,1-dicyanomethylene)-5-(tetrathiafulvalen-2-ylidene)-1,3-thiazole-4.

Introduction

Charge transfer (CT) studies seek to understand the ways in which their transfer rate of CT depends on the properties of the electro-donor and electro-acceptor system, solvent, molecular bridge and electronic coupling between the involved states^{1,2}. The different functionality played by these factors and the way they affect the qualitative and quantitative aspects of the electron transfer process have been extensively discussed in recent years³⁻⁷. The need for understanding the processes of electron (ET) or charge transfer at the molecular level have prompted the study of highly conjugated molecular systems of the donor-acceptor (D-A), type given their unique photo-physical and photo-activated properties⁸.

These properties have favoured the application and development of such systems in areas such as: non-linear optical materials⁹, molecular optical switches¹⁰, and photovoltaic cells¹¹, among others. In the field of photovoltaics, organic photovoltaic devices with D- π -A materials have attracted a lot attention due to their potential in the creation of flexible and remarkably light solar cells, with low manufacturing cost and high power conversion efficiency (PCE)¹². A key issue to understanding the CT process is the ability to make quantitative predictions and measurements of the characteristics associated to the individual molecular systems that allow useful information for a direct comparison of the electron dynamics inferred in electro and photochemistry, at the nanometric, molecular and electronic scales¹³.

Currently, the increasing availability of kinetic data of CT processes and the development of computational tools allow the study of different molecular systems independently of their size, that exhibit better photophysical properties, and facilitate a direct comparison between theory and experiment¹⁴⁻¹⁶. These systems consist of covalent bonds of electro-active

chemical species, whether they are electro-donors or electro-acceptors, which can be either connected through a π -conjugated bridge or directly. The derivatives of the Rhodanine implemented in the synthesis of push-pull systems are an example of these type of systems, and they have been used as an electro-acceptor fragment in a variety of organic compounds of interest; for example, in non-linear second order analytical reactivities, and, more recently, as metal-free organic dyes in the manufacturing of dyesensitized solar cells (DSSCs)^{17–19}. For this purpose, the push-pull molecular system of the donor-rhodanine type is efficiently anchored to the meso-porous surface of TiO_2 . The light absorbed by the dye injects electrons into the conduction band of the TiO_2 , thus generating an electric current, while the fundamental state of the dye is regenerated by the electrolyte²⁰.

The precise prediction of the electron transfer rate in chemical and biological reactions of this type makes them attractive systems for different applications in the field of molecular electronics^{21,22}. In this work, we present results obtained for new “push-pull” chromophores based on derivatives of rhodanine, whereby 4-dimethylamine and 2-formyltetraatetrafulvalene exhibit the role of electro-donor groups in which the nature of the electron transfer processes is studied when they are connected to a dicyanorhodanine electro-acceptor through a small molecular bridge. To determine the most stable structure, the absorption spectrum and the first electronic state of the complexes were calculated by means of density functional theory (DFT) numerical simulation. We study the way the character of electron transfer in complexes gets affected by the presence of a solvent that acts as an environment and also in gas phase, seeking to report on novel quantitative results for such compounds²³, and explore their potential in the application and design of innovative and highly efficient donor-acceptor multifunctional devices that exhibit optimal electronic properties.

Chromophores computational details

Here, consider the molecules (**Z**)-2-((1,1-dicyanomethylen)-5-(4-dimethylamino)benzylidene)-1,3-thiazole-4 (**molecule 1**), and (**Z**)-2-((1,1-dicyanomethylene)-5-(tetrathiafulvalen-2-ylidene)-1,3-thiazole-4 (**molecule 2**), as shown in Fig. 1. The geometries obtained for such most stable conformations (see Supplementary section) were used as input data for the full optimization of calculations of the ground state by means of the hybrid functional BE3LYP with a base set 6-31G+, using Gaussian 09²⁴; the corresponding optimized structures are used for the molecules energy calculation.

The molecules excited states were calculated by means of the time-dependent density functional theory (td-DFT), and the results here reported were carried out with the molecules i) in the gas phase, and ii) by simulating an environment—methanol as solvent. In order to see the effects caused by the solvent on the electronic properties of the different compounds, the working molecules in the solvent were designated as follows: system **S1**: Molecule 1 + Methanol and system **S2**: Molecule 2 + Methanol, while the system **GP1** : Molecule 1 in gas phase and the system **GP2**: Molecule 2 in gas phase. Additionally, different properties of these molecules, such as higher occupied molecular orbitals (HOMOs), lower unoccupied molecular orbitals (LUMOs), energy gap, reorganization energy, Gibbs free energy, and excitation energy are derived from the computational results.

In our theoretical calculations we take into account the effects due to the solvent, since we aim to make predictions about the experimental spectra with a reasonable precision. We consider methanol as solvent with $\epsilon = 32.6$, following a Conductor-like Polarization Continuum Model (C-PCM)^{25,26}.

Results and discussion

Electronic Transitions. Computational calculations to optimize the geometry of molecules **1** and **2** were carried out using DFT-B3LYP/6-31G+; subsequently we used td-DFT for de-

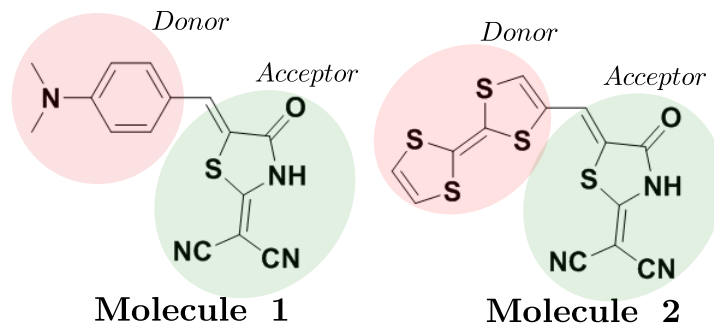


Figure 1: Molecular structure of the chromophores under study. Molecule 1 is the (**Z**)-2-((1,1-dicyanomethylen)-5-(4-dimethylamino)benzylidene)-1,3-thiazole-4, and molecule 2 is the (**Z**)-2-((1,1-dicyanomethylene)-5-(tetrathiafulvalen-2-ylidene)-1,3-thiazole-4.

terminating the transition states that most favoured the charge transfer and search for a favorable environment in the CT processes. The systems under study are of the donor-acceptor type in which two different electro-donor fragments are connected to an electro-acceptor fragment for generating an effective CT process, which results in a charge separation state for analyzing the key molecular properties in the calculation of the charge distributions in these molecules²³.

D- π -A molecular systems have two possible mechanisms for charge transfer, i) super exchange: the charge or electrons transferred do not reside directly in the molecular bridge and the states occupied by the molecule during this time are known as virtual excitations; and ii) sequential charge transfer (hopping): there are real intermediate states that are energetically accessible, and this (thermally activated) mechanism is generally more efficient for long-distance electronic transfer processes²⁷.

Here we analyze the frontier molecular orbitals in order to quantify the relationship between structural and electronic geometry. For system in solvent **S1**, the HOMO is mostly concentrated in the donor (4-dimethylamino group), while the HOMO-1 and the LUMO are mostly located in the acceptor (2-(1,1-dicyanomethylene)-1,3-thiazole-4), as seen in Fig. 2. Therefore, the CT is the charge transfer mixture within the 4-dimethylamino coupled with the CT from 2-(1,1-dicyanomethylene)-1,3-thiazole-4 to 4-dimethylamino moiety. For system **S2**, the HOMO and HOMO-1 are mainly located in the tetrathiafulvalene moiety,

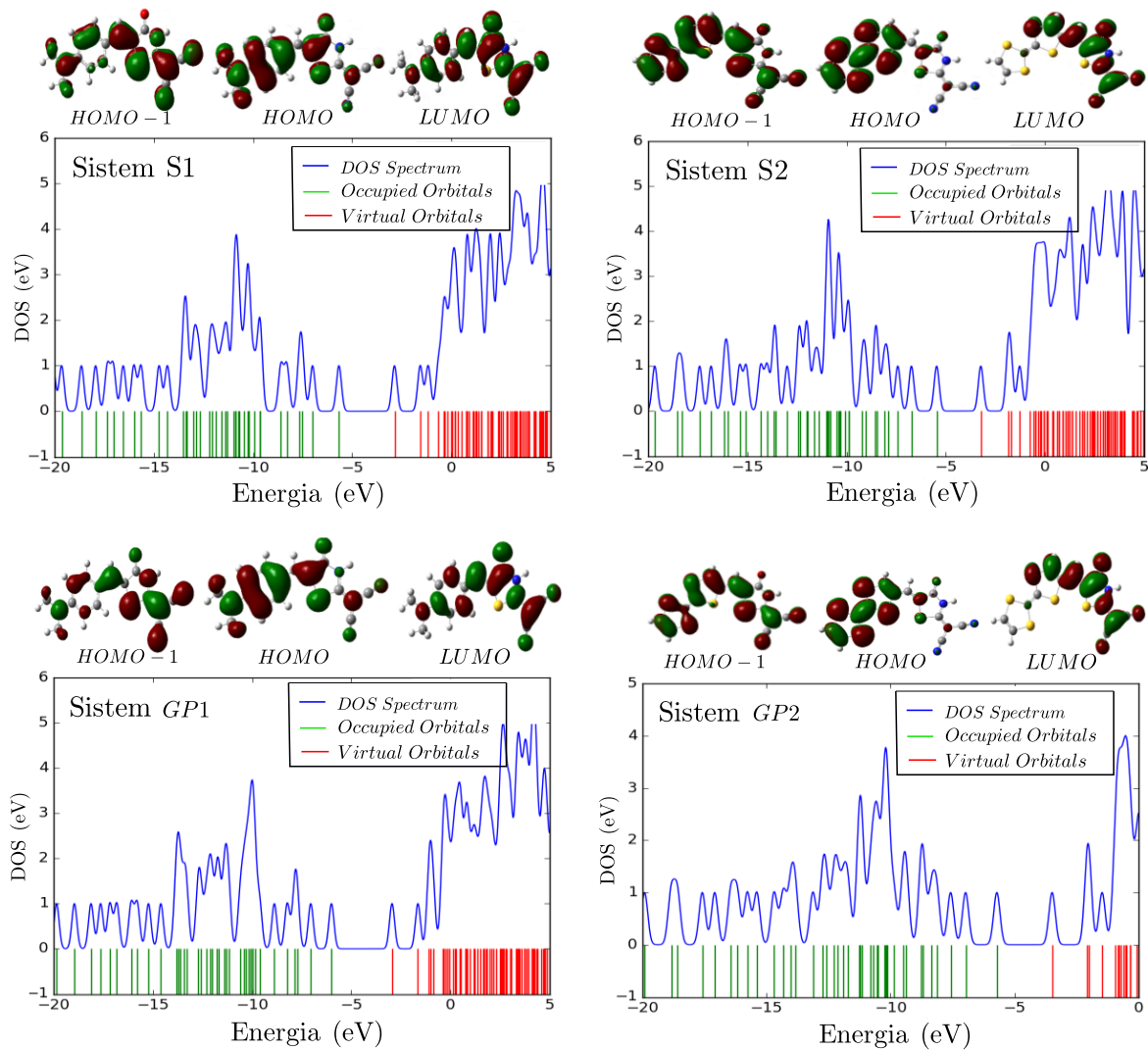


Figure 2: Spectra for the total density of states obtained using B3LYP/6-31G+ for the systems **S1**, **S2**, **GP1** and **GP2**. The blue curve represents the density of state spectrum, the green lines represent the occupied molecular orbitals, and the red lines are the virtual molecular orbitals.

while the LUMO is located in the 2-(1,1-dicyanomethylene)-1,3-thiazole-4 (Fig. 2). Thus, the transitions of system **S2** from the HOMO to the LUMO together with HOMO-1 to LUMO have a more significant character in the charge transfer with respect to system **S1**, reflecting that the tetrathiafulvalene acts as a better electro-donor fragment than the first one.

When we observe the frontier molecular orbitals of molecules in gas phase, we see that the behavior described above is maintained. However, their density of state spectra have very significative changes in the spectral densities corresponding to each energy level, which indicates a considerable effect due to the solvent on the electronic and geometric structure of the compounds.

Absorption Spectra. The electronic transition energies and the charge transfer transitions are calculated using TD-DFT/B3LYP^{28,29}. The UV-Vis absorption spectra for the systems **S1**, **S2**, **GP1** and **GP2** are shown in Fig. 3. We find that system **S1** has a strong absorption band at 490.01 nm, together with other bands of lower energy at 343.37 nm and 283.00 nm corresponding to transitions of the type $\pi - \pi^*$, which are associated to the S_2 and S_7 states, respectively (see Table 1). The intense high energy transition at 490.01 nm is described by the excitation HOMO→LUMO (99%), according to the orbital transition diagram (See Supporting information S1). This high energy transition can be assigned to intramolecular charge transfer from the 4-dimethylamino electro-donor fragment to the electro-donor fragment; the low energy transition at 343.37 nm corresponds to the transition HOMO→LUMO+1 (65%). The electronic transitions can be seen as a contribution to the intramolecular charge transfer process from the electro-donor to the electro-acceptor and like the low energy transition at 283.00 nm which is described by HOMO→LUMO+3 (75%).

The system **S2** shows a band of high energy absorption at 388.31 nm and bands of low absorption at 661.10 nm, 325.98 nm, and 294.66 nm. The low energy transition S_1 for the system **S2** is described by the transition HOMO→LUMO (99%), which represents an intramolecular CT from the 2-tetrathiafulvaleno electro-donor moiety to the 2-(1,1-

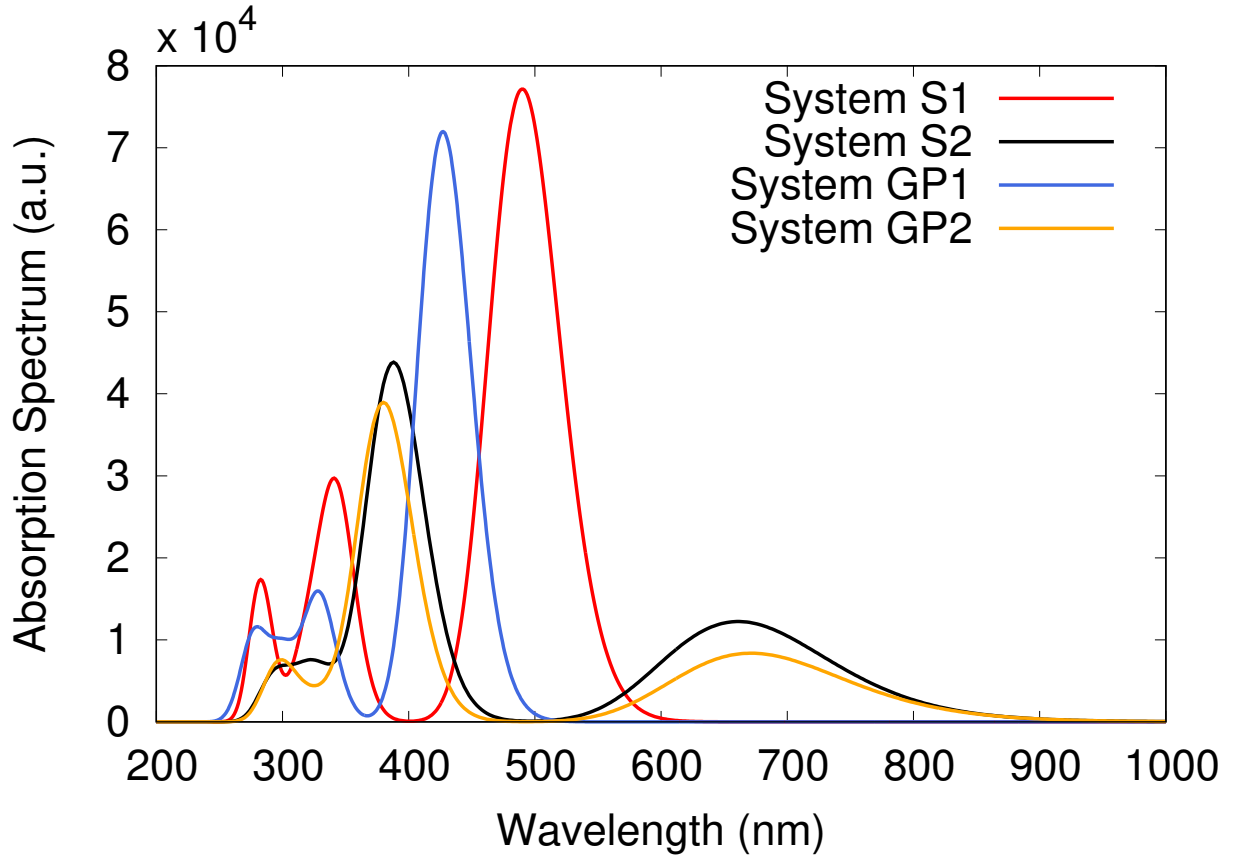


Figure 3: Absorption spectrum of the molecules in solvent (systems **S1**, **S2**), and molecules in gas phase (systems **GP1** and **GP2**).

Table 1: Wavelengths of the most important simulated transition states λ , oscillator strengths f_{os} , excitation energy E , and band gap energy ΔE_{H-L} .

| System | States | $\lambda(\text{nm})$ | ΔE_{H-L} (eV) | f_{osc} | E (eV) | Composition |
|------------|----------|----------------------|-----------------------|-----------|----------|----------------------------------|
| S1 | S_1 | 490.01 | 2.74 | 0.9727 | 2.530 | HOMO→LUMO (99%) |
| | S_2 | 343.37 | | 0.3391 | 3.611 | H-1→LUMO (%34); HOMO → L+1 (65%) |
| | S_7 | 283.00 | | 0.1336 | 4.381 | H-3→LUMO (16%);HOMO→L+3 (75%) |
| S2 | S_1 | 661.10 | 2.27 | 0.1995 | 1.875 | HOMO→LUMO (99%) |
| | S_4 | 388.31 | | 0.6559 | 3.193 | H-1→LUMO (88%); HOMO →L+1 (10%) |
| | S_6 | 325.98 | | 0.1099 | 3.803 | H-2→LUMO (92%) |
| | S_{10} | 294.66 | | 0.0962 | 4.208 | H-3→LUMO (80%); H-1 → L+1 (13%) |
| GP1 | S_1 | 427.12 | 3.05 | 0.9075 | 2.903 | HOMO→LUMO (99%) |
| | S_2 | 329.19 | | 0.1939 | 3.767 | H-1→LUMO (70%); HOMO → L+1 (29%) |
| | S_7 | 281.39 | | 0.0833 | 4.406 | H-2→LUMO (76%) |
| GP2 | S_1 | 671.27 | 2.23 | 0.1365 | 1.847 | HOMO→LUMO (99%) |
| | S_2 | 380.16 | | 0.6322 | 3.261 | H-1→LUMO (98%) |
| | S_3 | 297.93 | | 0.1194 | 4.161 | H-3→LUMO (79%); H-1 → L+1 (11%) |

dicianometilen)-1,3-tiazol-4 electro-acceptor fragment; for the case HOMO-1 and LUMO the latter mostly located in the 2-(1,1-dicianometilen)-1,3-tiazol-4 corresponds to the low transition energy of the state S_4 described by the transition HOMO-1 \rightarrow LUMO (88%) where a CT from electro-donor to electro-acceptor is present. For HOMO-3 and LUMO both mainly concentrated in 2- (1,1-dicyanomethylene)-1,3-thiazole-4, associated with the transition HOMO-3 \rightarrow LUMO (80%), a CT within the electro-acceptor and not a transfer from the electro-donor to the concise electro-acceptor takes place.

For the case of the system **GP1**, comprising the molecule **1** in gas phase, we observe that it presents a high energy absorption band at 427.12 nm corresponding to the transition state of the HOMO \rightarrow LUMO (99%). In addition, as in the case of the system **S1**, it presents two low energy absorption bands at i) 329.19 nm corresponding to the transition state of the HOMO-1 \rightarrow LUMO (70%) that describes a contribution to the process of CT in the interior of (2-(1,1-dicyanomethylene)-1,3-thiazol-4), since the HOMO-1 and LUMO are more concentrated in the acceptor, with a small CT contribution from the donor to the acceptor (as can be seen in Supporting information S2); and ii) a low energy band at 281.39 nm, corresponding to the transition of the HOMO-2 \rightarrow LUMO. By comparing the graphs of systems **S1** and **GP1**, we obtain that the solvent produces an effective shift or bathochromic displacement with respect to the wavelength of absorption.

The system **GP2** shows a similar behavior to that of system **S2**. However, a bathochromic shift is observed in relation to the absorption spectrum when comparing the systems **S2** and **GP2**. The resulting shift is associated to the molecule-solvent interaction, since for the system **GP2** this presents a high energy band at 380.16 nm, and for system **S2** in presence of methanol this occurs at 388.31 nm. In addition, the system **GP2** presents two low energy bands, one at 671.27 nm and the other one at 297.93 nm; they are associated with the transition states HOMO \rightarrow LUMO (99%), and HOMO-3 \rightarrow LUMO (79%), respectively. The energy band at 380.16 nm is associated to the transition status of HOMO-1 \rightarrow LUMO (98%).

Table 1 shows that f_{os} values, that correspond to the transition states HOMO \rightarrow LUMO

of systems **S1** and **GP1**, are similar to each other, as are for systems **S2** and **GP2**. The oscillation strength for an electronic transition is proportional to the transition dipole moment. In general, a large oscillator strength corresponds to large experimental absorption coefficients or a stronger fluorescence intensity³⁰. The results shown in Table 1 reveal that the systems **S1** and **GP1** correspond to systems that have a higher absorption capacity when compared to systems **S2** and **GP2**.

Emission Properties. We use td-DFT, with the hybrid B3LYP and basis set 6-31G+ in order to compute for the structure in an excited state and simulating the emission spectrum of the systems under study. The maximum emission wavelengths are shown in Table 2. The transitions $S_1 \rightarrow S_0$ and $S_3 \rightarrow S_0$ represent fluorescence peaks in the emission spectrum; in addition, the system **S1** has the highest oscillator strength, which corresponds to a LUMO→HOMO transition.

Table 2: Emission spectrum results obtained for the system under study in solvent (S) and gas phase (GP).

| System | Elect. Trans. | $\lambda_{max}(\text{nm})$ | $E_s(\text{eV})$ | f_{os} | Stokes Shift (nm) | $\tau_R(\text{ns})$ |
|------------|-----------------------|----------------------------|------------------|----------|----------------------|---------------------|
| S1 | $s_1 \rightarrow s_0$ | 508.90 | 2.4363 | 1.0126 | 18.0 | 3.85 |
| S2 | $s_3 \rightarrow s_0$ | 416.78 | 2.9748 | 0.5316 | 28.8 | 5.02 |
| GP1 | $s_1 \rightarrow s_0$ | 443.28 | 2.7970 | 0.918 | 16.2 | 3.36 |
| GP2 | $s_3 \rightarrow s_0$ | 415.36 | 2.9850 | 0.3792 | 35.2 | 7.29 |

The results for the excitation energy, oscillator strength and radiative lifetime are presented in Table 2. We also report the Stokes shift values, defined as the difference between λ_{max} of absorption and λ_{max} of emission spectrum. The Stokes shift gives the energy difference that exists between the absorption and emission due to the same levels. This provides information about the probability of radiative and non-radiative de-excitation between two levels, where the probability of radiative de-excitation increases with the difference of energy and that of the non-radiative decreases. Hence, the first one dominates when the energy levels are well separated and the second one does it when we have closer levels. Thus, the radiative lifetime was calculated for the spontaneous emission spectrum using the Einstein

transition probabilities according to the expression^{31,32}:

$$\tau_R = \frac{c^3}{2(E_{flu})^2 f_{osc}}, \quad (1)$$

where c is the speed of light in vacuum, E_{flu} is the fluorescence excitation energy, and f is the oscillator strength.

We conclude, as can be seen from Table 2 that the presence of the solvent favours the radiative processes for the case of molecule **1**, since the Stokes shift is greater in the presence of methanol (18.0 nm) than in the gas phase (16.2 nm). However, for the case of molecule **2** this process is favoured in the gas phase rather than in the presence of the solvent, which is made evident by the longer radiative lifetime found for the gas phase. It is well known that short radiative lifetimes lead to a high efficiency of light emission, while long radiative lifetime facilitates the electron and energy transfer. In our case, the radiative lifetime is shorter for systems with higher oscillator strength, which leads to an increase in luminescent efficiency.

The duration of emission (τ_R) for the studied molecules have the following order: $\tau_R^{GP2} > \tau_R^{S2} > \tau_R^{S1} > \tau_R^{GP1}$. This hierarchy indicates that the change of a donor unit strongly decreases the emission lifetime of the compound in both gas phase and solvent; we find the highest oscillator strength and the smallest lifetime radiation in the case of the system **S1** and **GP1**, which correspond to the molecule **1** under different environmental conditions. Consequently, molecule **1** represents a good emission material with high efficiency³³.

Charge Transfer Rate. Charge transfer is a crucial process involved in many physical and biology phenomena such as the photosynthesis³⁴; this process can be estimated, in a first approximation, by using the semi-classical theory of Marcus^{35,36}:

$$k_{e(h)} = \frac{2\pi}{\hbar} \frac{|V_{e(h)}|^2}{\sqrt{4\pi\lambda_{e(h)}k_B T}} \exp\left(-\frac{\lambda_{e(h)}}{4k_B T}\right), \quad (2)$$

where $V_{e(h)}$ is the electronic coupling between the final and the initial state for electrons

(holes), $\lambda_{e(h)}$ is the reorganization energy for electron (hole), and k_B denotes Boltzmann constant.

For an efficient CT mechanism the reorganization energy of the molecular system must be small and an electronic coupling between the electro-acceptor and electro-donor parts is necessary³⁷. The reorganization energy comprises two factors, the first one is the internal or intramolecular reorganization energy (λ_{int}), and the second one is the external or intermolecular reorganization energy (λ_{ext}). The λ_{int} accounts for the structural changes between neutral and ionic states and must be calculated, while λ_{ext} reflects the change in the polarization of the medium after the CT takes place³⁸.

The intramolecular reorganization energy λ_{int} can be estimated for the electrons (reorganization energy of electron λ_e) and for the holes (reorganization energy of holes λ_h), and can be expressed by the following equation^{39–41}:

$$\begin{aligned}\lambda_e &= \lambda_1^e + \lambda_2^e = (E_0^- - E_-^-) + (E_-^0 - E_0^0) \\ \lambda_h &= \lambda_1^h + \lambda_2^h = (E_0^+ - E_+^+) + (E_+^0 - E_0^0),\end{aligned}\quad (3)$$

where $E_0^+(E_0^-)$ is the energy of the cation (anion) calculated with the optimized structure of the neutral molecule. Similarly, E_+^+ is the energy of cation (anion) calculated with the optimized cation (anion) structure, E_+^0 (E_-^0) is the energy of the neutral molecule calculated at the cationic (anionic) state. Finally, E_0^0 is the energy of the neutral molecule at the ground state.

Table 3: Molecular calculation of the reorganization energy for electrons (holes) $\lambda_{e(h)}$, electronic coupling for the electron (holes) transfer mechanism $V_{e(h)}$, and electron (hole) transfer rate $k_{e(h)}$.

| System | λ_e (eV) | λ_h (eV) | V_e (eV) | V_h (eV) | $k_e(10^{15} \text{ s}^{-1})$ | $k_h(10^{15} \text{ s}^{-1})$ |
|------------|------------------|------------------|------------|------------|-------------------------------|-------------------------------|
| S1 | 0.1841 | 0.0942 | 0.660 | 0.685 | 2.870 | 5.13 |
| S2 | 0.3396 | 0.2190 | 0.700 | 0.620 | 0.528 | 1.67 |
| GP1 | 0.2708 | 0.1505 | 0.655 | 0.520 | 1.010 | 2.72 |
| GP2 | 0.3740 | 0.2211 | 0.720 | 0.630 | 0.371 | 1.61 |

This redistribution of energies for the case of electron reorganization energy is best observed in Fig. 4. The external reorganization energy λ_{ext} explains the nuclear shifts in the surrounding medium and the resulting electronic effects are much harder to calculate. This is assumed to be, for many authors, between 0.2 eV and 0.5 eV for simple models based on the dielectric properties of organic matrices^{42,43}.

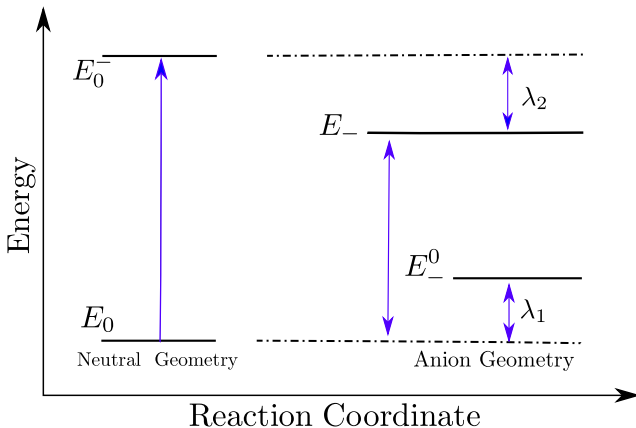


Figure 4: Scheme for the calculation of the reorganization energy for the electron transfer; λ_1 is the reorganization energy of the neutral molecule and λ_2 denote the reorganization energy of the radical anion.

We calculate the electron reorganization energy using Fig. 4. According to Marcus model, the rate of electron transfer depends mainly on the energy of reorganization and the coupling between the donor and the acceptor, in addition to the general exergonicity of the process³⁹. It is also considered that for a self-exchange electron transfer process (where interaction with solvent is not considered) the change in the Gibbs free energy is zero and the electron transfer rate will only depend intrinsically on the barrier of activation, marked by the internal and external reorganization energy, and the electronic coupling parameter V . The λ_{int} in Equ. (3) for the self-exchange process has two contributions, arising from the geometric relaxation along inter-nuclear coordinate upon moving from neutral-state to the charged-state geometry and vice versa.

The electronic coupling V , which is another important parameter in the CT process, is the geometrically most dependent element of the kinetic constant because its value depends

on the distance between donor-acceptor and the geometry of the system (orientation of the orbitals); this parameter is also sensitive to changes in the systems under study such as solvents, and temperature, among others⁴⁴⁻⁴⁷.

Here, we use the generalized Mulliken-Hush method (GMH)⁴⁸ to calculate the electronic couplings, and the operator used in the GMH method is the adiabatic dipole moment matrix μ_{12} ⁴⁸. Under this approach (and in the weak coupling regime), the electronic coupling for a direct donor-acceptor coupling is calculated by the equation⁴⁹:

$$V = \frac{\Delta E_{12}\mu_{12}}{\sqrt{(\Delta\mu_1 - \Delta\mu_2)^2 + 4\mu_{12}^2}}, \quad (4)$$

where ΔE_{12} is the orbital energy difference, and $\Delta\mu_{12}$ is the dipole moments difference of the adiabatic states.

The calculation of the reorganization energy, electronic coupling and the electron transfer rate are shown in Table 3. As reported in^{30,50,51}, it has been found that at low values of reorganization energy, the transfer rate is high. The hole reorganization energy calculated for the systems **S2** and **GP2** are smaller than those for the systems **S1** and **GP1**; this implies that the hole transfer rate is greater in the systems **S2** and **GP2**, and we also note that for the case of the system **S2** compared to the **GP2** the hole transport rate is higher in the presence of methanol than in the case of the gas phase, confirming this behavior for the case of the system **S1** and **GP1** where the same situation is observed, which indicates that methanol does not favour the transport of holes. Furthermore, the hole reorganization energies λ_h for all systems are smaller than that of N,N'-diphenyl-N,N'-bis(3-methylphenyl)-(1,10-biphenyl)-4,4'-diamine (TPD), which is a typical hole transport material with $\lambda_h = 0.290$ eV⁵². This implies that the hole transfer rates of the molecules **1** and **2**, in the condition under study, might be higher than that of TPD. Thus, the molecules **1** and **2** might comprise good hole transport materials from the stand point of the smaller reorganization energy. On the other hand, we observe that for the case of the system **S2** compared to **GP2** the hole transport rate is higher in the presence of methanol than in the case of the gas phase, confirming this

behavior for the case of the systems **S1** and **GP1** where the same situation occurs, which indicates that methanol favours the transport of voids.

The value of λ_e is smaller for the case of the systems **S1** and **GP1** than for the systems **S2** and **GP2**: this indicates that the electron transfer rates for **S1** and **GP1** will be larger than those due to the systems **S2** and **GP2** as can be seen in Table 3. In addition, by comparing λ_e for the systems **S1** and **GP1**, as well as for **S2** and **GP2**, we see that κ_e for $\kappa_e^{S1} > \kappa_e^{GP1}$ and κ_e in $\kappa_e^{S2} > \kappa_e^{GP2}$, which indicates that the electron transfer process is favoured by the presence of solvent in the molecules **1** and **2**. In addition, by comparing the reorganization energies for electron reorganization and holes, we observe that the values of λ_h are smaller than those for λ_e , suggesting that the carrier mobility of the electrons is larger than that of the holes. Hence, the molecules **1** y **2** can be used as promising hole transport materials in, e.g., organic light-emitting diodes from the stand point of the smaller reorganization energy, which can be corroborated with the κ values shown in the Table 3. Finally, given that κ_e and κ_h are greater for the systems **S1** and **GP1**, we conclude that the molecule **1** is better at transporting charge than the molecule **2**. In addition to the previous analysis, it can be seen that the molecule **1** is more transport-efficient than the molecule **2**.

Conclusions

We have theoretically investigated different optical and electronic properties for new structures based on 4-dimethylamino and tetrathiafulvalene as electro-donor groups and dicyanorhodanine as electro-acceptor group, in which the correlation between structures and electronic dynamics is studied by means of theoretical chemical calculations. It was observed that the presence of a solvent with which the molecules **1** and **2** interacts, favours the electronic transfer process. Furthermore, the change of the donor group shows that tetrathiafulvalene acts as a better electron donor than 4-dimethylamino. As regards the wavelength of absorption, this shows a bathochromic effect between the gas phase and the presence of the solvent. The computational results predict the electronic properties of the

systems **S1**, **S2**, **GP1** and **GP2**, and the analysis of the molecular frontier orbitals shows that the vertical electronic transitions of absorption of the studied compounds are characterized as intramolecular charge transfer. In addition, the molecules **1** and **2** can be used as void transport materials.

Acknowledgement

The authors acknowledge support by the Colombian Science, Technology and Innovation Fund-General Royalties System (Fondo CTeI-Sistema General de Regalías) under contract BPIN 2013000100007.

Supporting Information Available

The following files are available free of charge.

Contains the optimal geometries, the total energy and the frontier molecular orbitals involved in the electronic transitions at the TD-DFT B3LYP/6-31G+ levels.

References

- (1) Genereux, J. C.; Barton, J. K. Mechanisms for DNA charge transport. *Chemical reviews* **2009**, *110*, 1642–1662.
- (2) Delor, M.; Keane, T.; Scattergood, P. A.; Sazanovich, I. V.; Greetham, G. M.; Towrie, M.; Meijer, A. J.; Weinstein, J. A. On the mechanism of vibrational control of light-induced charge transfer in donor–bridge–acceptor assemblies. *Nature chemistry* **2015**, *7*, 689.
- (3) Nitzan, A. Electron transmission through molecules and molecular interfaces. *Annual Review of Physical Chemistry* **2001**, *52*, 681–750.

- (4) Zamadar, M.; Cook, A. R.; Lewandowska-Andralojc, A.; Holroyd, R.; Jiang, Y.; Bikalis, J.; Miller, J. R. Electron Transfer by excited benzoquinone anions: Slow rates for two-electron transitions. *The Journal of Physical Chemistry A* **2013**, *117*, 8360–8367.
- (5) Renaud, N.; Powell, D.; Zarea, M.; Movaghar, B.; Wasielewski, M. R.; Ratner, M. A. Quantum Interferences and Electron Transfer in Photosystem I. *The Journal of Physical Chemistry A* **2013**, *117*, 5899–5908.
- (6) Guan, L.; Mo, Y. Electron Transfer in Pnictogen Bonds. *The Journal of Physical Chemistry A* **2014**, *118*, 8911–8921.
- (7) Belmonte, D.; Gatti, C.; Ottonello, G.; Richet, P.; Vetuschi Zuccolini, M. Ab Initio Thermodynamic and Thermophysical Properties of Sodium Metasilicate, Na₂SiO₃, and Their Electron-Density and Electron-Pair-Density Counterparts. *The Journal of Physical Chemistry A* **2016**, *120*, 8881–8895.
- (8) Lee, W.-Y.; Kurosawa, T.; Lin, S.-T.; Higashihara, T.; Ueda, M.; Chen, W.-C. New donor–acceptor oligoimides for high-performance nonvolatile memory devices. *Chemistry of Materials* **2011**, *23*, 4487–4497.
- (9) Dragonetti, C.; Colombo, A.; Fontani, M.; Marinotto, D.; Nisic, F.; Righetto, S.; Roberto, D.; Tintori, F.; Fantacci, S. Novel Fullerene Platinum Alkynyl Complexes with High Second-Order Nonlinear Optical Properties as a Springboard for NLO-Active Polymer Films. *Organometallics* **2016**, *35*, 1015–1021.
- (10) Kanaani, A.; Ajloo, D.; Kiyani, H.; Amri, S. A. N. First-principles study of the electronic transport properties of a 1, 3-diazabicyclo [3.1. 0] hex-3-ene molecular optical switch. *Optik-International Journal for Light and Electron Optics* **2018**, *153*, 135–143.
- (11) Kesters, J.; Verstappen, P.; Raymakers, J.; Vanormelingen, W.; Drijkoningen, J.; D’Haen, J.; Manca, J.; Lutsen, L.; Vanderzande, D.; Maes, W. Enhanced organic so-

- lar cell stability by polymer (PCPDTBT) side chain functionalization. *Chemistry of Materials* **2015**, *27*, 1332–1341.
- (12) Hedley, G. J.; Ruseckas, A.; Samuel, I. D. Light harvesting for organic photovoltaics. *Chemical Reviews* **2016**, *117*, 796–837.
- (13) Abendroth, J. M.; Bushuyev, O. S.; Weiss, P. S.; Barrett, C. J. Controlling motion at the nanoscale: rise of the molecular machines. *ACS nano* **2015**, *9*, 7746–7768.
- (14) Ferretti, A. Theory of electroabsorption spectroscopy in poly-nuclear Ru complexes. *Coordination Chemistry Reviews* **2003**, *238*, 127–141.
- (15) Cacelli, I.; Campanile, S.; Denti, G.; Ferretti, A.; Sommovigo, M. [(NH₃)₅Ru (1, 2, 4, 5-tetrazine)]²⁺: Synthesis and Experimental and Theoretical Study of Its Solvatochromism in the Visible Spectral Region. *Inorganic Chemistry* **2004**, *43*, 1379–1387.
- (16) Prytkova, T. R.; Kurnikov, I. V.; Beratan, D. N. Coupling coherence distinguishes structure sensitivity in protein electron transfer. *Science* **2007**, *315*, 622–625.
- (17) Kuang, D.; Uchida, S.; Humphry-Baker, R.; Zakeeruddin, S. M.; Grätzel, M. Organic Dye-Sensitized Ionic Liquid Based Solar Cells: Remarkable Enhancement in Performance through Molecular Design of Indoline Sensitizers. *Angewandte Chemie* **2008**, *120*, 1949–1953.
- (18) Zhang, M.-D.; Huang, C.-Y.; Song, M.-X.; Zhao, D.-X.; Cao, H.; Chen, M.-D. D-D- π -A organic dye containing rhodanine-3-acetic acid moiety for dye-sensitized solar cells. *Mendeleev Communications* **2016**, *26*, 288 – 290.
- (19) Zhu, B.-y.; Wu, L.; Ye, Q.; Gao, J.-r.; Han, L. Asymmetric double donor- π -acceptor dyes based on phenothiazine and carbazole donors for dye-sensitized solar cells. *Tetrahedron* **2017**, *73*, 6307–6315.

- (20) Liang, M.; Xu, W.; Cai, F.; Chen, P.; Peng, B.; Chen, J.; Li, Z. New triphenylamine-based organic dyes for efficient dye-sensitized solar cells. *The Journal of Physical Chemistry C* **2007**, *111*, 4465–4472.
- (21) Nar, H.; Messerschmidt, A.; Huber, R.; van de Kamp, M.; Canters, G. W. Crystal structure analysis of oxidized *Pseudomonas aeruginosa* azurin at pH 5.5 and pH 9.0: A pH-induced conformational transition involves a peptide bond flip. *Journal of Molecular Biology* **1991**, *221*, 765–772.
- (22) Page, C. C.; Moser, C. C.; Chen, X.; Dutton, P. L. Natural engineering principles of electron tunnelling in biological oxidation–reduction. *Nature* **1999**, *402*, 47–52.
- (23) Insuasty, A.; Ortiz, A.; Tigreros, A.; Solarte, E.; Insuasty, B.; Martín, N. 2-(1, 1-dicyanomethylene) rhodanine: a novel, efficient electron acceptor. *Dyes and Pigments* **2011**, *88*, 385–390.
- (24) Frisch, M.; Trucks, G.; Schlegel, H.; Scuseria, G.; Robb, M.; Cheeseman, J.; Scalmani, G.; Barone, V.; Mennucci, B.; Petersson, G. Gaussian 09, Revision A. 02; Gaussian, Inc: Wallingford, CT, 2009. *Gaussian 09, Revision A. 02; Gaussian, Inc: Wallingford, CT*, 2013.
- (25) Takano, Y.; Houk, K. Benchmarking the conductor-like polarizable continuum model (CPCM) for aqueous solvation free energies of neutral and ionic organic molecules. *Journal of Chemical Theory and Computation* **2005**, *1*, 70–77.
- (26) Chiu, K. Y.; Govindan, V.; Lin, L.-C.; Huang, S.-H.; Hu, J.-C.; Lee, K.-M.; Tsai, H.-H. G.; Chang, S.-H.; Wu, C.-G. DPP containing D– π –A organic dyes toward highly efficient dye-sensitized solar cells. *Dyes and Pigments* **2016**, *125*, 27–35.
- (27) Ortiz, A.; Insuasty, B.; Illescas, B. M.; León, N. M. Transferencia electrónica y nanocables moleculares orgánicos. *Anales de la Real Sociedad Española de Química*. 2008; pp 270–275.

- (28) Ganji, M. D.; Hosseini-Khah, S.; Amini-Tabar, Z. Theoretical insight into hydrogen adsorption onto graphene: a first-principles B3LYP-D3 study. *Physical Chemistry Chemical Physics* **2015**, *17*, 2504–2511.
- (29) Ganji, M. D.; Tajbakhsh, M.; Kariminasab, M.; Alinezhad, H. Tuning the LUMO level of organic photovoltaic solar cells by conjugately fusing graphene flake: A DFT-B3LYP study. *Physica E: Low-dimensional Systems and Nanostructures* **2016**, *81*, 108–115.
- (30) Sun, F.; Jin, R. DFT and TD-DFT study on the optical and electronic properties of derivatives of 1, 4-bis (2-substituted-1, 3, 4-oxadiazole) benzene. *Arabian Journal of Chemistry* **2017**, *10*, S2988–S2993.
- (31) Hlel, A.; Mabrouk, A.; Chemek, M.; Khalifa, I. B.; Alimi, K. A DFT study of charge-transfer and opto-electronic properties of some new materials involving carbazole units. *Computational Condensed Matter* **2015**, *3*, 30–40.
- (32) Bourass, M.; Benjelloun, A. T.; Benzakour, M.; Mcharfi, M.; Hamidi, M.; Bouzzine, S. M.; Bouachrine, M. DFT and TD-DFT calculation of new thienopyrazine-based small molecules for organic solar cells. *Chemistry Central Journal* **2016**, *10*, 67.
- (33) Zhang, Y.; Zhang, L.; Wang, R.; Pan, X. Theoretical study on the electronic structure and optical properties of carbazole- π -dimesitylborane as bipolar fluorophores for nondoped blue OLEDs. *Journal of Molecular Graphics and Modelling* **2012**, *34*, 46–56.
- (34) Gray, H. B.; Winkler, J. R. Electron flow through proteins. *Chemical Physics Letters* **2009**, *483*, 1–9.
- (35) Marcus, R. A. Electron transfer reactions in chemistry. Theory and experiment. *Reviews of Modern Physics* **1993**, *65*, 599.
- (36) Marcus, R. A. Chemical and electrochemical electron-transfer theory. *Annual Review of Physical Chemistry* **1964**, *15*, 155–196.

- (37) Coropceanu, V.; Cornil, J.; da Silva Filho, D. A.; Olivier, Y.; Silbey, R.; Brédas, J.-L. Charge Transport in Organic Semiconductors. *Chemical Reviews* **2007**, *107*, 926–952, PMID: 17378615.
- (38) Li, Y.; Qi, D.; Sun, C.; Zhao, M. Spectra and charge transport of polar molecular photoactive layers used for solar cells. *Journal of Chemistry* **2015**, *2015*.
- (39) Pandith, A. H.; Islam, N. Electron transport and nonlinear optical properties of substituted arylidimesityl boranes: a DFT study. *PloS one* **2014**, *9*, e114125.
- (40) Kose, M. E.; Long, H.; Kim, K.; Graf, P.; Ginley, D. Charge transport simulations in conjugated dendrimers. *The Journal of Physical Chemistry A* **2010**, *114*, 4388–4393.
- (41) DeVine, J. A.; Labib, M.; Harries, M. E.; Rached, R. A. M.; Issa, J.; Wishart, J. F.; Castner Jr, E. W. Electron-Transfer Dynamics for a Donor–Bridge–Acceptor Complex in Ionic Liquids. *The Journal of Physical Chemistry B* **2015**, *119*, 11336–11345.
- (42) Olivier, Y.; Muccioli, L.; Lemaire, V.; Geerts, Y.; Zannoni, C.; Cornil, J. Theoretical characterization of the structural and hole transport dynamics in liquid-crystalline phthalocyanine stacks. *The Journal of Physical Chemistry B* **2009**, *113*, 14102–14111.
- (43) Kose, M. E.; Long, H.; Kim, K.; Graf, P.; Ginley, D. Charge transport simulations in conjugated dendrimers. *The Journal of Physical Chemistry A* **2010**, *114*, 4388–4393.
- (44) Kaniyankandy, S.; Rawalekar, S.; Sen, A.; Ganguly, B.; Ghosh, H. N. Does bridging geometry influence interfacial electron transfer dynamics? case of the enediol-TiO₂ system. *The Journal of Physical Chemistry C* **2011**, *116*, 98–103.
- (45) Li, H.; Brédas, J.-L.; Lennartz, C. First-principles theoretical investigation of the electronic couplings in single crystals of phenanthroline-based organic semiconductors. *The Journal of Chemical Physics* **2007**, *126*, 164704.

- (46) Valeev, E. F.; Coropceanu, V.; da Silva Filho, D. A.; Salman, S.; Brédas, J.-L. Effect of electronic polarization on charge-transport parameters in molecular organic semiconductors. *Journal of the American Chemical Society* **2006**, *128*, 9882–9886.
- (47) Mallick, G.; Karna, S. P.; He, H.; Pandey, R. Length-dependence of electron transfer coupling matrix in polyene wires: Ab initio molecular orbital theory study. *International Journal of Quantum Chemistry* **2009**, *109*, 1302–1310.
- (48) Cave, R. J.; Newton, M. D. Generalization of the Mulliken-Hush treatment for the calculation of electron transfer matrix elements. *Chemical Physics Letters* **1996**, *249*, 15–19.
- (49) Li, Y.; Feng, Y.; Sun, M. Photoinduced charge transport in a BHJ solar cell controlled by an external electric field. *Scientific Reports* **2015**, *5*, 13970.
- (50) Ran, X.-Q.; Feng, J.-K.; Ren, A.-M.; Li, W.-C.; Zou, L.-Y.; Sun, C.-C. Theoretical study on photophysical properties of ambipolar spirobifluorene derivatives as efficient blue-light-emitting materials. *The Journal of Physical Chemistry A* **2009**, *113*, 7933–7939.
- (51) Zou, L. Y.; Ren, A. M.; Feng, J. K.; Liu, Y. L.; Ran, X. Q.; Sun, C. C. Theoretical study on photophysical properties of multifunctional electroluminescent molecules with different π -conjugated bridges. *The Journal of Physical Chemistry A* **2008**, *112*, 12172–12178.
- (52) Gruhn, N. E.; da Silva Filho, D. A.; Bill, T. G.; Malagoli, M.; Coropceanu, V.; Kahn, A.; Brédas, J.-L. The vibrational reorganization energy in pentacene: molecular influences on charge transport. *Journal of the American Chemical Society* **2002**, *124*, 7918–7919.

Graphical TOC Entry

